Acta Biochim Biophys Sin 2012, 44: 241–248 | © The Author 2012. Published by ABBS Editorial Office in association with Oxford University Press on behalf of the Institute of Biochemistry and Cell Biology, Shanghai Institutes for Biological Sciences, Chinese Academy of Sciences. DOI: 10.1093/abbs/gmr126.
Advance Access Publication 10 January 2012

Original Article

The combined influence of surface modification, size distribution, and interaction time on the cytotoxicity of CdTe quantum dots in PANC-1 cells

Shuquan Chang, Bin Kang, Xiqin Liu, Yaodong Dai*, and Da Chen*

College of Material Science and Technology, Nanjing University of Aeronautics and Astronautics, Nanjing 210016, China
*Correspondence address. Tel: +86-25-52112903; Fax: +86-25-52112626; E-mail: Yd_dai@sina.com (Y.D.)/Tel: +86-25-84895988; Fax: +86-25-84892914; E-mail: Dachen@nuaa.edu.cn (D.C.)

Mercaptopropionic acid (MPA) and cysteamine (Cys) capped CdTe quantum dots (QDs) were successfully prepared and used to investigate the combined influence of surface modification, size distribution, and interaction time on their cytotoxicity in human pancreatic carcinoma (PANC-1) cells. Results indicated that the smaller the size of MPA-CdTe QDs, the higher the cytotoxicity, which could be partly due to the difference of their distribution inside cells. Comparing with MPA-CdTe QDs, Cys-CdTe QDs had better cellular metabolizability and lower cytotoxicity. These QDs' cellular distribution and cytotoxicity were closely related to their interaction time with cells. Their cytotoxicity was found to be significantly enhanced with the increase of incubation time in medium. After QD treatments, the influence of recover time on the final cell viability was also dependent on the concentration and surface modification of QDs used in pretreatment. The combined influence of these factors discussed here might provide useful information for understanding and reducing the cytotoxicity of QDs in future biomedical applications.

Keywords quantum dot; cytotoxicity; human pancreatic carcinoma cell; combined influence

Received: October 5, 2011 Accepted: November 24, 2011

Introduction

With the rapid development of nanotechnology, numerous nanomaterials have been widely used in biomedical areas [1,2]. Quantum dots (QDs) have been gaining popularity due to their potential applications in cellular imaging and medical diagnosis [3,4]. How to evaluate and minimize the cytotoxicity of QDs is still a great challenge for their clinical applications [5–8]. Many *in vitro* studies have been done to evaluate the toxicity of QDs in different types of cells. MUA-QD/SSA complexes (0.4 mg/ml) did not exhibit obvious influence on the viability of Vero cells [9]. The toxicity of QDs was dependent not on the nanocrystal itself but rather on the surface molecules [10]. Green CdTe QDs showed higher cytotoxicity than red ones, which might be influenced by their surface coatings [11,12]. In 2006, Hardman published a comprehensive review regarding the toxicology of QDs and concluded that the toxicity of QDs was mainly dependent on QD size, surface charge, concentration, outer coating bioactivity (capping material and functional groups), and oxidative, photolytic, and mechanical stability [13]. CdTe QDs and CdSe/ZnS QDs coated with the same molecules also exhibited distinct cytotoxicity [14]. The cytotoxicity of CdSe/ZnS QDs with different coatings in HEK cells was investigated. Results showed that 20 nM QDs coated with carboxylic acid resulted in a significant loss of cell viability by 24 h, however QDs coated with PEG in the same concentration had no effect on the cell viability [15]. The hippocampal neuronal cells treated with 1 nM CdSe QDs for 24 h showed no decrease in cell viability; however, the viability of cells treated with 10 and 20 nM QDs decreased by 20% and 30%, respectively, under the same conditions [16]. Our previous work revealed that the cytotoxicity of silk fibroin coated CdSe QDs was obviously lower than the thioglycolic acid coated ones in human pancreatic carcinoma (PANC-1) cells [17]. Our another study indicated that green and red mercaptopropionic acid capped CdTe (MPA-CdTe) QDs exhibited different cellular distribution and ultraviolet (UV)-enhanced cytotoxicity in PANC-1 cells [18]. Recently, the endothelial toxicity of mercaptosuccinic acid-capped CdTe QDs (0.1–100 μg/ml) was examined, which revealed that 0.1 μg/ml QDs also exhibited cytotoxicity [19]. Till now, many studies have been carried out to investigate the cytotoxicity of QDs and many novel results have been achieved. However, there are still many unclear processes and inconsistencies among different researchers, which might mainly be attributed to the broad diversity of QDs and the complexity of biological systems [20].

As mentioned above, many factors could influence the cytotoxicity of QDs, so they should be considered

comprehensively. Previous studies primarily focused on the analysis of simplex influence factor. Here, different size MPA-CdTe and cysteamine-capped CdTe (Cys-CdTe) QDs were prepared and characterized. The morphological changes and metabolic activity of PANC-1 cells containing QDs under different conditions (particle sizes, surface coating, incubating time in medium containing QDs, recover time in the fresh medium after QDs treatments) were examined and the combined influence of these factors was discussed in detail.

Materials and Methods

Preparation and characterization of MPA-CdTe and Cys-CdTe QDs

All reagents used in this study were analytical grade and purchased from Sigma-Aldrich Company (St Louis, USA) unless indicated otherwise. MPA-CdTe and Cys-CdTe QDs were synthesized as the method described in previous literatures [12]. Different size MPA-CdTe QDs (QD_{538}, QD_{561}, QD_{580}, QD_{605}, and QD_{629}) were formed after different reaction time from 10 min to 7 h. The prepared QDs solution was dialyzed against deionized water for 6 h and concentrated using a rotary evaporator. QDs were collected by centrifugation and purified by size-selective precipitation.

The physicochemical properties of as-obtained CdTe QDs were examined subsequently. Photoluminescence spectra were measured with a HITACHI 850 spectrofluorophotometer (Tokyo, Japan). Photographs were taken under UV illumination and sun light, respectively. The particle sizes and ξ-potentials were determined using Malvern Nano-ZS90 zetasizer (Westborough, USA) and JEOL JEM-200CX transmission electron microscope (Tokyo, Japan).

Cell culture and QDs treatment

PANC-1 cells (#TIB-222; ATCC, Manassas, USA) were cultured in DMEM medium containing 10% (*v*/*v*) fetal calf serum at 37°C in humidified air containing 5% CO_2. For fluorescence microscopic measurements, cells should be seeded onto a glass coverslip placed in six-well plates. For 3-(4,5-dimethylthiazol-2-yl)-2,5-diphenyl tetrazolium bromide (MTT) assays, cells were cultured in 96-well plates. Cells were incubated up to ~24 h and grown to ~80% confluence before experiments. QDs dispersed in PBS were added to each well to achieve a final concentration. Cells were then incubated in these medium containing QDs at 37°C in 5% CO_2 atmosphere for different time periods. After incubation with QDs, cells were washed with PBS to remove excess QDs and placed in fresh solutions before the subsequent experiments. All treatments were done in triplicates or quadruplicates in three or more independent experiments.

Laser scanning confocal microscopy

Olympus FV-1000 laser scanning confocal microscope (LSCM; Tokyo, Japan) was used to acquire images. After the treatments, PANC-1 cells were fixed with 4% paraformaldehyde for 15 min, and then washed three times with PBS buffer. To clearly observe the distribution and positions of QDs in cells, nuclei were stained with 0.1 μg/ml 4′,6-diamidino-2-phenylindole (DAPI) for 2 min. Before imaging, cells were washed with PBS again. Three channels (CH1: excitation 405 nm, filter 420–470 nm; CH2: excitation 488 nm, different filter for different QDs; CH3: 405/488 nm, Dic) were set to record DAPI, QDs, and Dic signals. Cells were observed using ×60 oil immersion objective. Images were acquired at a resolution of 800 × 800, and the scan size was 212 × 212 μm.

Cytotoxicity assay

MTT assays were performed to assess the metabolic activity of cells treated under different conditions. After the treatments, the medium was removed and replaced with serum-free media (200 μl/well). A total of 20 μl stock MTT (5 mg/ml) was added to each well, and the cells were then incubated for 1 h at 37°C. The medium was removed, and the cells were lysed with dimethyl sulfoxide. The absorbance was measured at 595 nm.

Results

Characterization of MPA-CdTe QDs and Cys-CdTe QDs

The structure schematic diagrams of MPA-CdTe and Cys-CdTe QDs were shown in **Fig. 1(a)**. Both MPA-CdTe

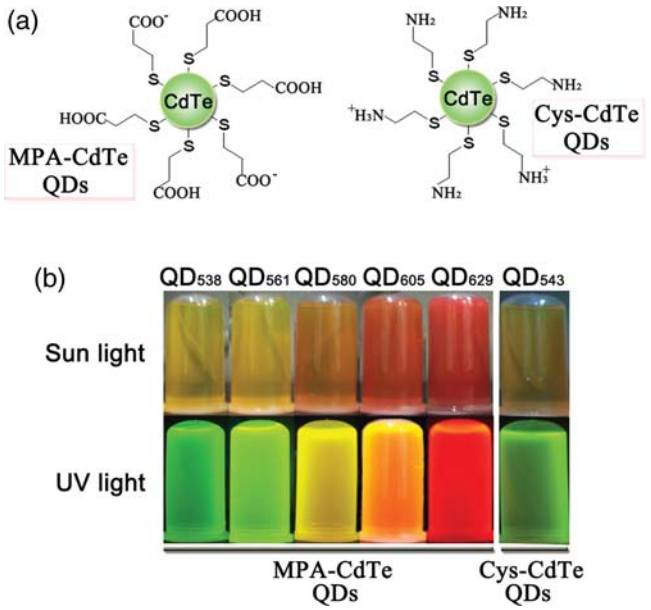

Figure 1 Structure schematic diagrams (a) and photographs (b) of MPA-CdTe QDs and Cys-CdTe QDs The photographs of QDs were taken under UV illumination and sun light, respectively.

and Cys-CdTe QDs exhibited excellent water solubility and bright fluorescence under UV illumination [**Fig. 1(b)**]. The smaller-size MPA-CdTe QDs emitted shorter wavelength light than the lager ones (**Table 1**). The ξ-potentials of MPA-CdTe QDs and Cys-CdTe QDs were negative and positive, respectively (**Table 1**).

Table 1 Physicochemical properties of CdTe QDs used in this study

Name	Coatings	Photoluminescence wavelength (nm)	Average size (nm)	ξ-potential (mV)
QD_{538}	MPA	538	2.7	−36.6
QD_{561}	MPA	561	3.6	−38.1
QD_{580}	MPA	580	4.3	−38.8
QD_{605}	MPA	605	5.2	−37.1
QD_{629}	MPA	629	6.0	−39.2
QD_{543}	Cys	543	2.8	+21.7

Distinct cellular distribution of QDs and morphological changes of PANC-1 cells containing QDs under different conditions

Five kinds of MPA-CdTe QDs could be successfully delivered into PANC-1 cells, but different QDs exhibited distinct cellular distribution (**Fig. 2**). The most striking difference about the localization between smaller-size QDs and larger-size ones in was observed in the nuclear vs. cytoplasmic compartments. PANC-1 cells treated with green QDs (QD_{538}) showed that some QDs were located in the cytoplasm and a few QDs appeared in the nuclei [**Fig. 2(f,k)**]. In contrast, most of red QDs (QD_{629}) distributed throughout the cytoplasm but no red QD was observed in the nuclei [**Fig. 2(j,l)**], which was consistent with the previous reports [11]. The cellular distribution of QD_{561}, QD_{580}, and QD_{605} [**Fig. 2(g–i)**] was shown between the states of QD_{538} and QD_{629}. These results indicated that smaller-size QDs were easier to transfer into cells and nuclei. The particle sizes of QDs were considered

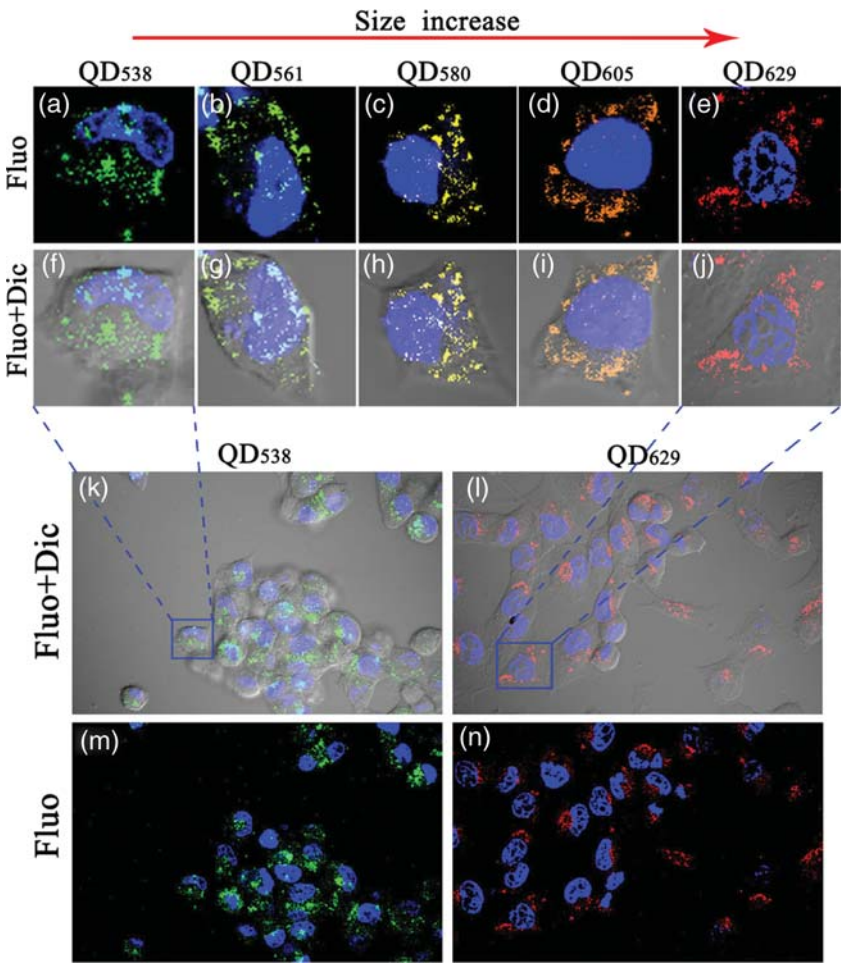

Figure 2 LSCM images of PANC-1 cells incubated with different sized MPA-CdTe QDs (a–e) Fluorescence images of cells incubated with QD_{538}, QD_{561}, QD_{580}, QD_{605}, and QD_{629}. (f–j) The overlay images of (a–e) and Dic images, respectively. (m,n) Low-resolution fluorescence images of cells incubated with QD_{538} and QD_{629}. (k,l) The overlay images of (m,n) and Dic images, respectively. Cells were incubated with QDs (20 μg/ml) for 4 h, and then LSCM imaging were carried out immediately. Nuclei were stained by DAPI.

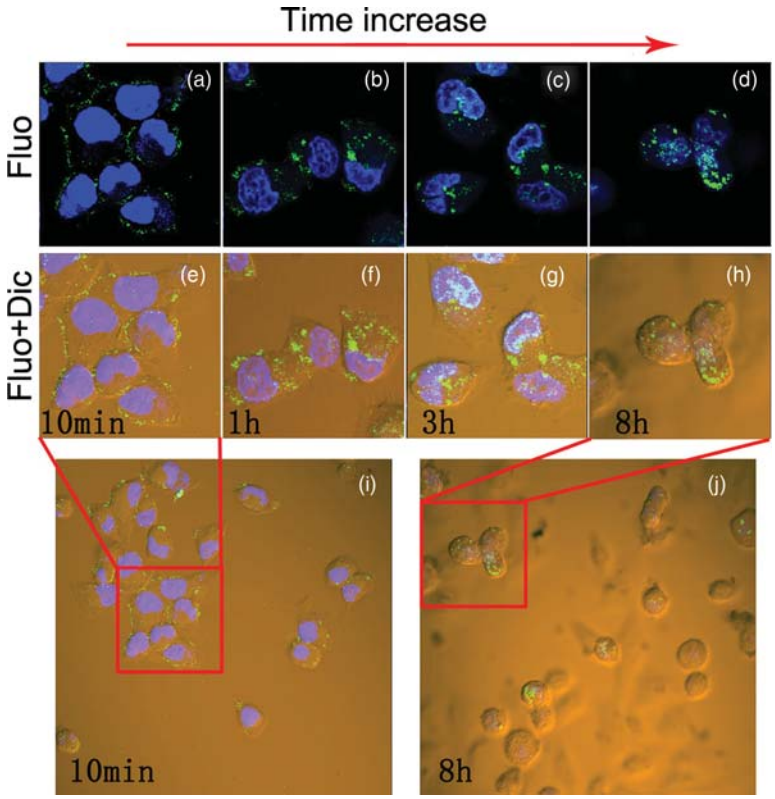

Figure 3 LSCM images of PANC-1 cells incubated with MPA-CdTe QDs for different time (a–d) Fluorescence images of cells incubated with QD_{538} for 10 min, 1 h, 3 h, and 8 h. (e–h) The overlay images of (a–d) and Dic images, respectively. (i,j) Low-resolution images of (e,h), respectively. Cells were incubated with QD_{538} (20 μg/ml) for different time, and then LSCM imaging were carried out immediately. Nuclei were stained by DAPI.

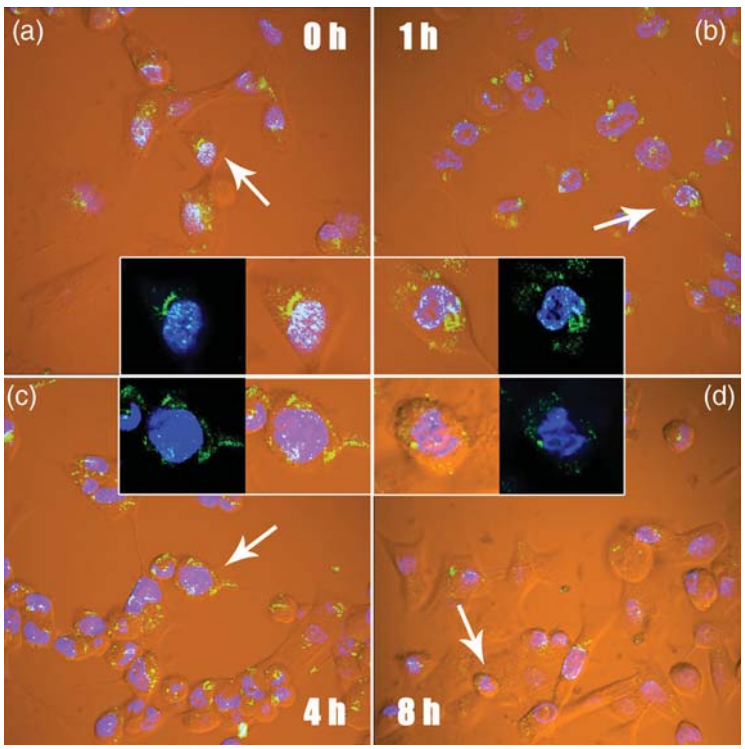

Figure 4 LSCM images of PANC-1 cells incubated in fresh medium for different time after QDs treatments (a–d) The overlay images of fluorescence and Dic images of PANC-1 cells incubated in fresh medium for 0, 1, 4, and 8 h after QDs treatments. Insets in (a–d) showed the magnified image of a certain cell. Cells were incubated with QD_{538} (20 μg/ml) for 4 h, and then cells were incubated in fresh medium for different time before LSCM imaging. Nuclei were stained by DAPI.

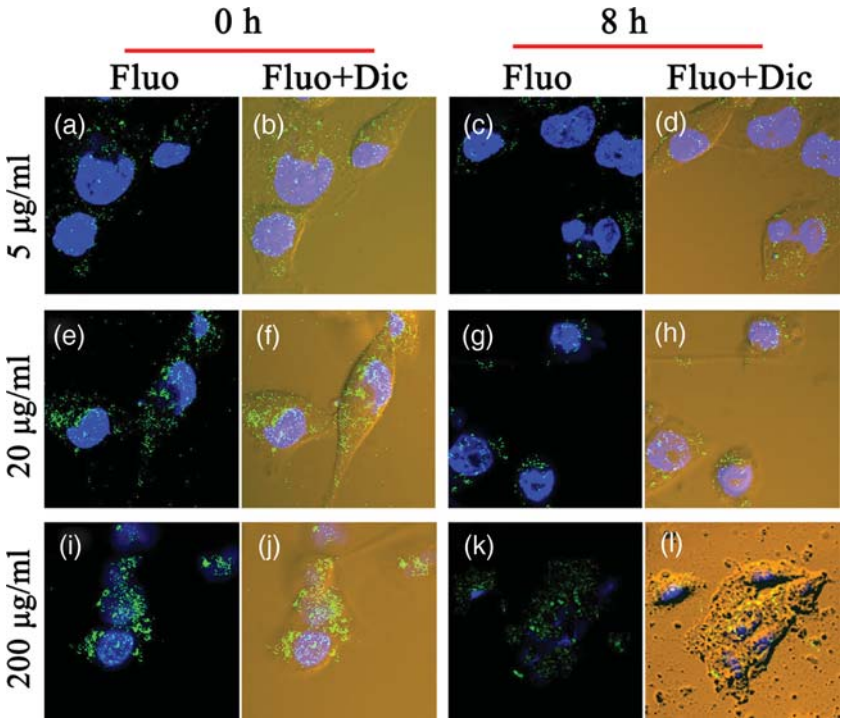

Figure 5 LSCM images of PANC-1 cells incubated in fresh medium for 0 and 8 h after different concentration QDs treatment (a,c) Fluorescence images of cells treated with 5 μg/ml QD_{538}. (b,d) The overlay images of (a,c) and Dic images, respectively. (e,g) Fluorescence images of cells treated with 20 μg/ml QD_{538}. (f,h) The overlay images of (e,g) and Dic images, respectively. (i,k) Fluorescence images of cells treated with 200 μg/ml QD_{538}. (j,l) The overlay images of (a,c) and Dic images, respectively. Cells were incubated with QD_{538} for 4 h, and then cells were incubated in fresh medium for 0 or 8 h before LSCM imaging. Nuclei were stained by DAPI.

very important to their cellular metabolizability, distribution, and cytotoxicity.

MPA-CdTe QDs were successfully taken up by cells and presented different cellular distribution depending on the incubation time with QDs (**Fig. 3**). QDs were mostly adhered on the cellular membrane and barely found inside the cells at the beginning (10 min). With the increase of incubation time (1 h), most of the QDs appeared in cells and were located in the cytoplasm around the nuclei. When the incubation time reached 3 h, QDs appeared in the nuclei. If the incubation time continued to prolong, QDs in cells seemed to decrease and changes of cellular morphology occurred. The incubation time of cells in medium containing QDs might influence the cytotoxicity of QDs, which would be discussed in the next section.

With the increase of recover time in fresh medium after QDs treatments, QDs in cells especially in nuclei seemed to decrease and changes of cellular morphology occurred [**Fig. 4(a–c)**]. When the incubation time reached 8 h, the amount of QDs in cells was obviously reduced and the integrality of cells began to be destroyed [**Fig. 4(d)**]. When the final concentration of MPA-CdTe QDs (QD_{538}) in medium was 5 μg/ml, the amount of QDs in cells obviously decreased but the cellular morphology showed no visible changes when the recover time in fresh medium reached 8 h [**Fig. 5(d)**], comparing with that at 0 h [**Fig. 5(b)**]. When the concentration of QDs in medium was 20 μg/ml, the QDs in cells decreased and the cellular morphology showed minor changes with the increase of recover time in fresh medium [**Fig. 5(f,h)**]. If the final concentration of QDs in medium reached 200 μg/ml, the amount of QDs in cells was also obviously reduced and the integrality of cells was seriously destroyed after incubation in fresh medium for 8 h [**Fig. 5(j,l)**]. Above results revealed that the recover time in fresh medium after QDs treatments could affect the metabolizability and the damage level of QDs in cells, which was related to the concentration and properties of QDs in medium.

QD_{538}, QD_{543}, and QD_{629} showed different cellular distribution and metabolic behavior (**Fig. 6**). With the increase of incubation time with QDs in medium, QDs were gradually delivered into cells and located in different positions, which is related to their particle sizes and coatings [**Fig. 6(a–n)**]. Smaller-size MPA-CdTe QDs (QD_{538}) were easier to transfer into cells and nuclei than the larger ones (QD_{629}), which was consistent with the results in **Fig. 2**. The particle sizes of Cys-CdTe QDs (QD_{543}) and MPA-CdTe QDs (QD_{538}) were almost the same (**Table 1**). However, more QD_{543} were taken up by cells than QD_{538} when the incubation time was 3 h [**Fig. 6(l,n)**]. With the increase of recover time in fresh medium after QDs treatments, the cellular distribution of QDs and the morphology of PANC-1 cells containing QDs were changed step by

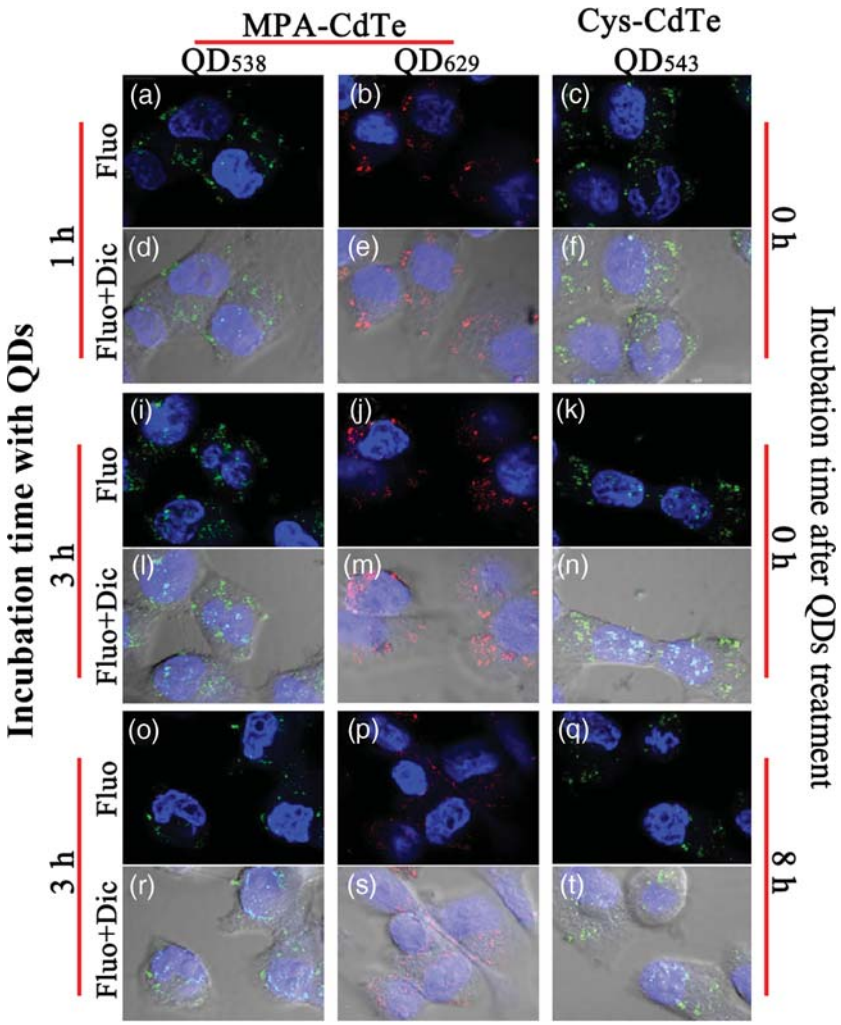

Figure 6 The combined influence of size distribution, surface modification, and interaction time on cellular distribution of QDs and morphological of PANC-1 cells containing QDs (a–c) Fluorescence images of cells treated in QD_{538}, QD_{629}, QD_{543} medium for 1 h and incubated in fresh medium for 0 h after QDs treatment. (d–f) The overlay images of (a–c) and Dic images, respectively. (i–k) Fluorescence images of cells treated in QD_{538}, QD_{629}, QD_{543} medium for 3 h and incubated in fresh medium for 0 h after QDs treatment. (l–n) The overlay images of (i–k) and Dic images, respectively. (o–q) Fluorescence images of cells treated in QD_{538}, QD_{629}, QD_{543} medium for 3 h and incubated in fresh medium for 8 h after QDs treatment. (r–t) The overlay images of (o–q) and Dic images, respectively. Cells were incubated with QDs (20 μg/ml) for 1 or 3 h, and then cells were incubated in fresh medium for 0 or 8 h before LSCM imaging. Nuclei were stained by DAPI.

step, which was also affected by the particle sizes and coatings of QDs [**Fig. 6(n–t)**]. QD_{543} in cells and nuclei were less than QD_{538} when the recover time after QDs treatments was 8 h [**Fig. 6(r,t)**]. Above results revealed that Cys-CdTe QDs (QD_{543}) were easier to be delivered into or out of cells, which might mainly be attributed to their different surface modification. The influences of size distribution, surface modification, interaction time on cellular distribution, and metabolic ability of QDs were interrelated.

Metabolic activity of PANC-1 cells treated with QDs of different sizes, coatings, and interaction time

Based on above observed distinct cellular distribution of QDs and changes of cell morphology, MTT assays were carried out to investigate the cytotoxicity of QDs under different conditions. With the increase of MPA-CdTe QDs sizes, the metabolic activities of cells were increased correspondingly (**Fig. 7**). When the concentration of QDs in medium was 20 μg/ml, the metabolic activity of cells treated with QD_{538}, QD_{561}, QD_{580}, QD_{605}, and QD_{629} was ~28%, ~31%, ~35%, ~38%, and ~41%, respectively. When the concentration of QDs in medium was 5 μg/ml, the trends were similar. The metabolic activity of cells treated with 20 μg/ml QD_{543} was ~38%, which was ~10% higher than QD_{538}. Cys-CdTe QDs exhibited lower cytotoxicity than MPA-CdTe QDs.

When the incubation time was 0.2 h, the metabolic activity of cells containing QD_{538}, QD_{629}, and QD_{543} was all >90%, which showed no visible cytotoxicity (**Fig. 8**). When the incubation time was increased to 5 h, the metabolic activity of cells containing QD_{538}, QD_{629}, and QD_{543} reduced to 58%, 64%, and 60%, respectively. If the

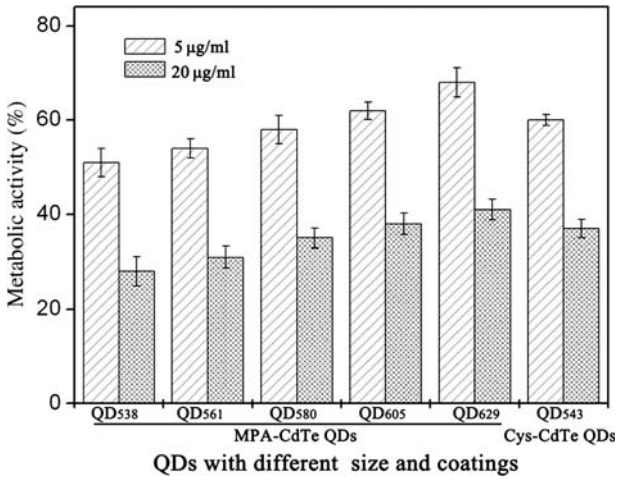

Figure 7 The metabolic activity of PANC-1 cells treated with different sized and coatings QDs Cells were incubated with QDs (5 or 20 μg/ml) for 10 h, and then MTT assays were carried out immediately. Data were presented as the mean ± standard deviation for three independent experiments.

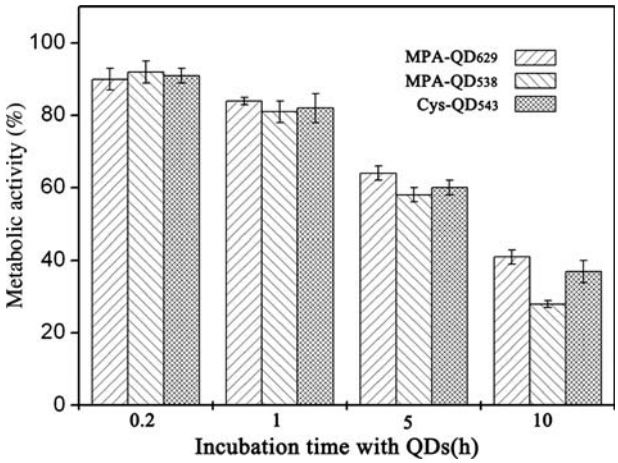

Figure 8 The metabolic activity of PANC-1 cells treated with QDs for different time Cells were incubated with QDs (20 μg/ml) for different time, and then MTT assays were carried out immediately. Data were presented as the mean ± standard deviation for three independent experiments.

incubation time reached 10 h, the metabolic activity of cells containing three kinds of QDs was all decreased to <45%. These results revealed that the cytotoxicity of QDs was enhanced with the increase of incubation time with containing QDs.

When the concentration of QDs was 5 μg/ml, the metabolic activity of cells showed increasing trends with the increase of recover time in fresh medium after QDs treatments (**Fig. 9**). When the concentration of QDs was 20 or 200 μg/ml, the metabolic activity of cells was gradually decreased with the increase of incubation time after QDs treatments. With the increase of incubation time after QDs treatments, the metabolic activity of cells treated with

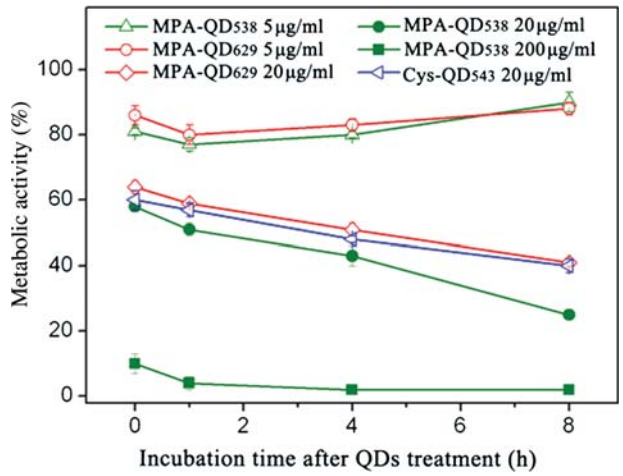

Figure 9 The influences of size distribution, surface modification, and interaction time on metabolic activity of PANC-1 cells treated with QDs Cells were incubated with QDs (5, 20, or 200 μg/ml) for 4 h, and then cells were incubated in fresh medium for different time before MTT assays. Data were presented as the mean ± standard deviation for three independent experiments.

smaller-size QD_{538} reduced faster than those treated with larger-size QD_{629}. When the incubation time was prolonged, the metabolic activity of cells treated with 20 μg/ml Cys-CdTe QDs (QD_{543}) reduced more slowly than those treated with MPA-CdTe QDs (QD_{538}). When the concentration of QDs reached 200 μg/ml, the metabolic activity of cells dropped rapidly to near zero with the increase of incubation time after QD treatments.

Discussion

There are many factors that can influence the cellular distribution and the damage level of QDs. Those factors are often interrelated, so they should be considered comprehensively. Herein, we mainly demonstrated the combined influence of surface modification, size distribution, and interaction time on the cytotoxicity of CdTe QDs in PANC-1 cells.

Different size QDs exhibited distinct cellular distribution and cytotoxicity (**Figs. 2** and **7**). The larger-size QDs could be delivered into cells and distributed throughout the cytoplasm, but no QD was observed in the nuclei. In contrast, the smaller-size QDs were easier to be transferred into cells and nuclei. Nuclei were considered as one of the most sensitive cellular organelles. QDs in nuclei might more directly and seriously induce damage to DNA or other targeting molecules. So, the smaller-size QDs could induce more serious damages to cells and exhibited higher cytotoxicity. Similar-size QDs with different coatings exhibited different metabolic behavior and cytotoxicity (**Figs. 6** and **9**). Cys-CdTe QDs were easier to be delivered into or out of cells than MPA-CdTe ones, which might be attributed to their distinct surface potentials. The surface of Cys-CdTe QDs had

many amino groups that could be ionized in solution and was electropositive. Electropositive Cys-CdTe QDs were easier to interact with the electronegative cellular surface. The surface of MPA-CdTe QDs was electronegative, which made them difficult to contact with cellular surface. Cys-CdTe QDs exhibited lower cytotoxicity, which might relate to the high metabolizability and reactive oxygen species eliminate the effects of amino groups. QDs presented different cellular distribution depending on the incubation time with QDs (**Fig. 3**). The uptake and distribution of QDs in cells need a period of time and should undergo a complex process. QDs firstly adhered to the cell membrane, the first step of interaction with cells; and then entered cells and located in cytoplasm around nuclei; subsequently they could be delivered into nuclei if their sizes were small enough [12,21]. As mentioned above, the location of QDs in cells would affect the damage level to cells. So, the incubation time with QDs was an important factor on the cytotoxicity of QDs (**Fig. 8**). With the increase of incubation time, QDs were gradually absorbed and transferred into important cellular organelles, which would usually bring more and more obvious damages to the targeting cells. The metabolizability and cytotoxicity of QDs was also influenced by the recover time in fresh medium after QDs treatments (**Figs. 4**, **5**, and **9**). When the concentration of QDs was very low, the initial damage to cells was minor and usually could be self-repaired with the cellular metabolism. If the concentration of QDs was high, the initial damage was too serious to be repaired by themselves, which would trigger the cellular processes of the apoptosis or cell death. The size distribution, surface modification concentration, and incubating time with QDs would jointly decide if the damage could be self-repaired or worsened with the increase of incubation time in fresh medium.

The biological system is very complex and the structure of QDs is also diverse. So, the cytotoxicity of QDs could be affected by many factors. A deeper understanding of combined influence and mechanism of cytotoxicity might be very meaningful to promote the applications of QDs in biomedical areas.

Funding

This work was supported by the grants from the National Natural Science Foundation of China (11105073, 81101146, 81071256), the China Postdoctoral Science Foundation (20100471338), the Natural Science Foundation of Jiangsu Province (BK2011739, BK2011738), and the NUAA Research Funding (NS2010152).

References

1 Nel A, Xia T, Madler L and Li N. Toxic potential of materials at the nanolevel. Science 2006, 311: 622–627.

2 Barreto JA, O'Malley W, Kubeil M, Graham B, Stephan H and Spiccia L. Nanomaterials: applications in cancer imaging and therapy. Adv Mater 2011, 23: H18–H40.

3 Michalet X, Pinaud FF, Bentolila LA, Tsay JM, Doose S, Li JJ and Sundaresan G, *et al*. Quantum dots for live cells, in vivo imaging, and diagnostics. Science 2005, 307: 538–544.

4 Medintz IL, Uyeda HT, Goldman ER and Mattoussi H. Quantum dot bioconjugates for imaging, labelling and sensing. Nat Mater 2005, 4: 435–446.

5 Jaiswal JK, Mattoussi H, Mauro JM and Simon SM. Long-term multiple color imaging of live cells using quantum dot bioconjugates. Nat Biotechnol 2003, 21: 47–51.

6 Wu XY, Liu HJ, Liu JQ, Haley KN, Treadway JA, Larson JP and Ge NF, *et al*. Immunofluorescent labeling of cancer marker Her2 and other cellular targets with semiconductor quantum dots. Nat Biotechnol 2003, 21: 41–46.

7 Parak WJ, Boudreau R, Le Gros M, Gerion D, Zanchet D, Micheel CM and Williams SC, *et al*. Cell motility and metastatic potential studies based on quantum dot imaging of phagokinetic tracks. Adv Mater 2002, 14: 882–885.

8 Sanjeev KM, Chansik P, Tae HY and Seog WR. Assessment of cytocompatibility of surface-modified CdSe/ZnSe quantum dots for BALB/3T3 fibroblast cells. Toxicol in Vitro 2010, 24: 1070–1077.

9 Hanaki K, Momo A, Oku T, Komoto A, Maenosono S, Yamaguchi Y and Yamamoto K. Semiconductor quantum dot/albumin complex is a long-life and highly photostable endosome marker. Biochem Biophys Res Commun 2003, 302: 496–501.

10 Hoshino A, Fujioka K, Oku T, Suga M, Sasaki YF, Ohta T and Yasuhara M, *et al*. Physicochemical properties and cellular toxicity of nanocrystal quantum dots depend on their surface modification. Nano Lett 2004, 4: 2163–2169.

11 Lovric J, Bazzi HS, Cuie Y, Fortin GRA, Winnik FM and Maysinger D. Differences in subcellular distribution and toxicity of green and red emitting CdTe quantum dots. J Mol Med 2005, 83: 377–385.

12 Lovric J, Cho SJ, Winnik FM and Maysinger D. Unmodified cadmium telluride quantum dots induce reactive oxygen species formation leading to multiple organelle damage and cell death. Chem Biol 2005, 12: 1227–1234.

13 Hardman R. A toxicologic review of quantum dots: toxicity depends on physicochemical and environmental factors. Environ Health Persp 2006, 114: 165–172.

14 Cho SJ, Maysinger D, Jain M, Roder B, Hackbarth S and Winnik FM. Long-term exposure to CdTe quantum dots causes functional impairments in live cells. Langmuir 2007, 23: 1974–1980.

15 Ryman-Rasmussen JP, Riviere JE and Monteiro-Riviere NA. Surface coatings determine cytotoxicity and irritation potential of quantum dot nanoparticles in epidermal keratinocytes. J Invest Dermatol 2007, 127: 143–153.

16 Tang ML, Xing TR, Zeng J, Wang HL, Li CC, Yin ST and Yan D, *et al*. Unmodified CdSe quantum dots induce elevation of cytoplasmic calcium levels and impairment of functional properties of sodium channels in rat primary cultured hippocampal neurons. Environ Health Persp 2008, 116: 915–922.

17 Chang SQ, Dai YD, Kang B, Han W and Chen D. Gamma-radiation synthesis of silk fibroin coated CdSe quantum dots and their biocompatibility and photostability in living cells. J Nanosci Nanotechnol 2009, 9: 5693–5700.

18 Chang SQ, Dai YD, Kang B, Han W, Mao L and Chen D. UV-enhanced cytotoxicity of thiol-capped CdTe quantum dots in human pancreatic carcinoma cells. Toxicol Lett 2009, 188: 104–111.

19 Yan M, Zhang Y, Xu KD, Fu T, Qin HY and Zheng XX. An *in vitro* study of vascular endothelial toxicity of CdTe quantum dots. Toxicology 2011, 282: 94–103.

20 Pelley JL, Daar AS and Saner MA. State of academic knowledge on toxicity and biological fate of quantum dots. Toxicol Sci 2009, 112: 276–296.

21 Maysinger D. Nanoparticles and cells: good companions and doomed partnerships. Org Biomol Chem 2007, 5: 2335–2342.